

# Electrical and Structural Design of Air-conditioning Fan Motor for Noise Reduction

**Hyung Suk Han, Jin Yong Mo, Chang Hyun Kim, Jae Kwon Lee**

*Air-conditioning Technical Expert Group, System Appliance Division, Samsung Electronics,  
416, Metan-3dong, Yeongtong-Gu, Suwon, Korea*

**Weui Bong Jeong\***

*Department of Mechanical Engineering, Pusan National University,  
Jangjeon-dong, Kumjung-ku, Pusan 609-735, Korea*

AC induction motors have been widely used for fan motor of the air conditioner indoor unit. Noise of these AC induction motors is usually caused by the coupling effects of structural and electrical systems. The rotating torque and the noise from AC induction motor were discussed in this paper. First, the modification of motor was carried out in order to reduce the unbalance magnetomotive force between main and sub winding. Second, structural modification based on normal mode analysis and modal testing was carried out so that the fan motor does not have the natural frequencies near the 2f-line frequency. Numerical modifications through these two processes were verified by experiments, which showed that the sound pressure level at 2f-line frequency of the modified system became about 25dB less than that of conventional one.

**Key Words:** 2f-Line Frequency, Resonance, Induction Motor, Magnetomotive Force, Forced Vibration

## 1. Introduction

Nowadays, air conditioners have been becoming more necessary and having various functions in a real life. With the elevation of standards for a living, consumer's requirements for an air conditioner become severe for low noise as well as high performance. For the fan motor of air conditioner indoor unit, the low noise requirement is grown up continuously. So many studies have been performed in these days in order to reduce this kind of noise.

Williams and Smith (1999) and Yang (2001) studied to reduce motor vibration for either elec-

trical point of view or structural point of view. Yang dealt with resonance problem of BLDC fan motor related to the inserted length of the shaft to the fan. Willam R. Finley (2000) summarized the vibration problems of induction motor related to motor design, which referred that motor noise problem comes from electrical problems as well as structure ones. For the electrical problem, he dealt with electrical imbalance such as magnetic flux variation by different air gap and loosening lamination of the core, and for the mechanical problems, he dealt with them such as resonance, critical speed, misalignment and mechanical imbalance. Yang (1998) performed a study for reducing motor vibration considering motor torque and structural resonance coupling effect of the rotor. Transient vibration analysis of a rotary compressor was conducted by Jeong (2002) considering motor torque according to compressor load as well as mechanical force for moving parts.

In this paper, the torque produced by induction motor was modeled and estimated. The param-

---

\* Corresponding Author,

**E-mail:** wbjeong@pusan.ac.kr

**TEL:** +82-51-510-2337; **FAX:** +82-51-517-3805

Department of Mechanical Engineering, Pusan National University, Jangjeon-dong, Kumjung-ku, Pusan 609-735, Korea. (Manuscript **Received** February 15, 2006;

**Revised** July 10, 2006)

---

ters of equivalent circuit of induction motor were identified by experiments. In an electrical point of view, the parameters of motor were modified in order to reduce the unbalance magnetomotive force between main and sub winding. In a structural point of view, the structural modification based on normal mode analysis and modal testing were also carried out in order for the fan motor not to have the natural frequencies near the 2f-line frequency. The electrical and structural modifications by computational analysis were compared to experimental results in order to verify the usefulness of computational analysis.

## 2. Electrical Design of Fan Motor for Reducing 2f-Line Frequency Noise

Motor used in this study is a single-phase 8 poles 50 Hz permanent split-phase type capacitor induction motor for package air conditioner indoor unit and fan type is sirocco. The mathematical model of the motor torque and the relationship between distribution of the magnetomotive force and motor noise will be discussed.

### 2.1 Torque modeling of capacitor split-phase type induction motor

The torque of AC power supply electric motor can be expressed as follows :

$$\begin{aligned}
 T &= 1/\omega_{syn} I_2^2 R_2/s \\
 &= R_2/\omega_{syn} I_2^2 \cos^2(\omega t) \\
 &= 0.5 R_2/\omega_{syn} I_2^2 (1 + \cos(2\omega t)) \\
 &= K_e (1 + \cos(2\omega t))
 \end{aligned}
 \tag{1}$$

Here,  $T$  is a torque of the motor,  $\omega_{syn}$  is synchronous speed,  $I_2$  is rotor induced current,  $R_2$  is rotor resistance,  $\omega$  is line frequency and  $K_e$  is constant of torque. It can be seen that motor torque has pulsation according to two times frequency for line voltage. In this paper, this two times frequency will be called 2f-line frequency.

In order to model the torque produced by capacitor split phase motor, equivalent circuit for motor was applied as shown in Fig. 1. No-load and locking test for main and sub winding of the motor were conducted in order to get the constant

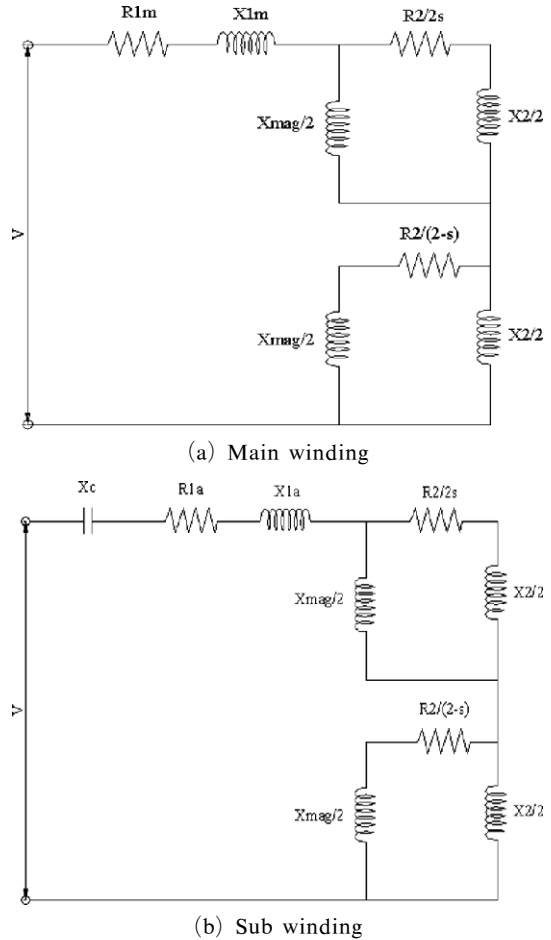


Fig. 1 Equivalent circuit of induction motor

values of the equivalent circuit. It is necessary to determine torque constant,  $K_e$ , in order to model the torque  $T$  in Eq. (1), which was estimated by experiment from equivalent circuit given in Fig. 1. From 2-revolution flux theory (Sen, 1997) and symmetry coordinate system law (Sen, 1997), the main winding and sub winding equivalent circuits of the induction motor can be expressed separately as shown in Fig. 1. Figure 1 (a) represents equivalent circuit for main winding, while  $R_{1m}$  denotes main coil resistance,  $X_{1m}$  denotes main coil leakage reactance,  $R_2$  denotes rotor resistance,  $X_2$  denotes rotor leakage reactance,  $X_{mag}$  denotes magnetize reactance of rotor and  $s$  denotes slip. Figure 1(b) represents equivalent circuit for sub winding. Here,  $R_{1a}$  denotes sub coil resistance,  $X_{1a}$  denotes sub coil leakage

**Table 1** Test results of the motor

Test items	Input voltage (V)	Line Frequency (Hz)	Input current (I)	Power (W)
No load Test	220	50	0.53	115.0
Locking Test for Main coil	50	50	0.38	15.6
Locking Test for Sub coil	50	50	0.37	14.95

**Table 2** Equivalent circuit constants of motor identified from test results

Parameters	symbol	value	Unit
slip	s	1.0	—
main coil resistance	R1m	32.0	$\Omega$
sub coil resistance	R1a	23.2	$\Omega$
capacitor	Xc	212.2	$\Omega$
rotor resistance	R2	76.0	$\Omega$
main coil leakage reactance	X1m	37.6	$\Omega$
sub coil leakage reactance	X1a	42.0	$\Omega$
rotor leakage reactance	X2	37.6	$\Omega$
rotor magnetize reactance	Xmag	300.0	$\Omega$

reactance and  $X_c$  denotes capacitor reactance ( $=1/2\pi fC$ ). The equivalent circuit constants were identified by experiments as given in Tables 1 and 2. Through locking test for main coil,  $X_{1m}$  and  $X_2$  could be identified. And  $X_{1a}$  could be identified with locking test for sub coil, and  $X_{mag}$  could be identified with no load test for sub coil (Hubert, 2002 ; Sen, 1997).

Average torque of electric motor estimated by equivalent circuit can be expressed as follows :

$$T = [\{ I_m^2 + (aI_a)^2 \} (R_f - R_b) + 2aI_mI_a (R_f + R_b) \sin(a)] / \omega_{syn} \quad (2)$$

Here,  $I_m$  is current of main coil,  $I_a$  is current of sub coil,  $a$  is turn ratio ( $=N_a/N_m$ ),  $R_f$  is forward direction ingredient of rotor resistance ( $=R_2/2s$ ),  $R_b$  is backward direction ingredient of rotor resistance ( $=R_2/(2-s)$ ),  $a$  is phase angle of main coil current and sub coil current and  $\omega_{syn}$  is synchronous speed. The motor torque versus rpm from Eq. (2) was given in Fig. 2. The slip is 0.2 and torque is 43 kgf-cm since motor rpm at fan normal load is 600 RPM. The value of  $Ke$  in Eq.(1) is driven as 25.19 kgf-cm in order that the

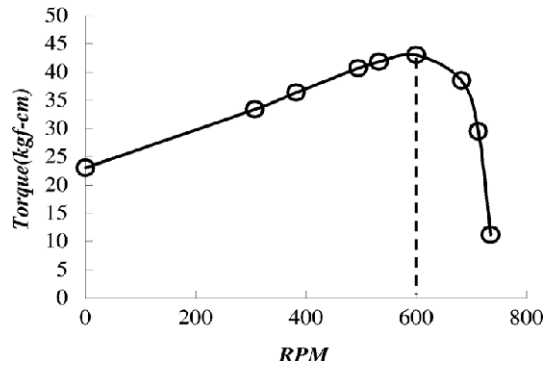


**Fig. 2** Speed-Torque curve identified from Eq. (2)

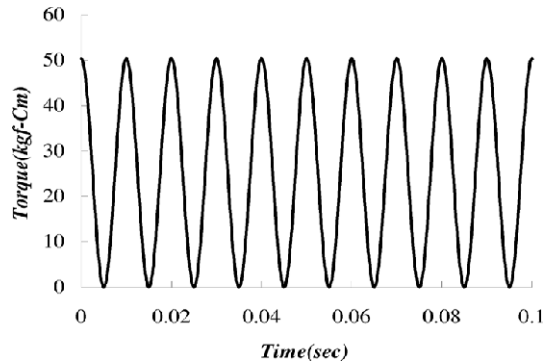


**Fig. 3** Torque of induction motor ( $Ke=25.19$  kgf-cm)

torque from Eq. (1) is equal to that from Eq. (2) at  $s=0.2$ . The torque variation versus time was given in Fig. 3.

**2.2 Magnetomotive force of capacitor split phase motor**

AC induction motor used widely for household appliance is usually permanent split-phase type induction motor which is given in Fig. 4. In the case of general single-phase motor, rotating force doesn't arise if the power is supplied without

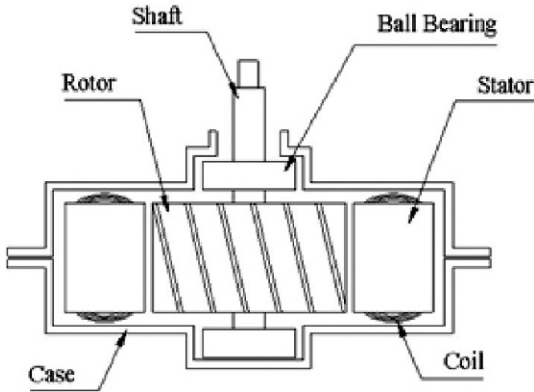
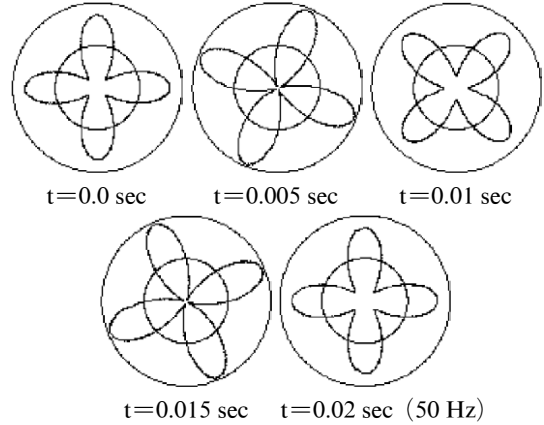


Fig. 4 Schematic diagram of capacitor split phase induction motor

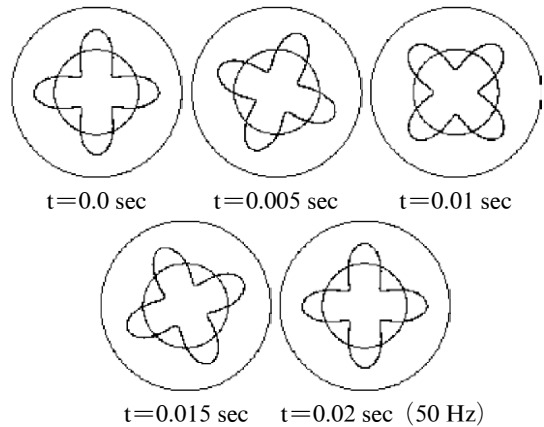
starter because revolutionary flux is occurred equally for forward and backward rotating direction. However, if it moves, the forward and backward flux will be different, and be acted as an unbalance two-phase motor. At this time, magnetomotive force could be expressed as Eq. (3) (Sen, 1997).

$$\begin{aligned}
 F(\theta, t) &= F_m(\theta, t) + F_a(\theta, t) \\
 &= N_m i_m \cos \theta + N_a i_a \cos(\theta + 90^\circ) \\
 &= \sqrt{2} N_m I_m \cos \omega t \cos \theta \\
 &\quad + \sqrt{2} N_a I_a \cos(\omega t + \theta_a) \cos(\theta + 90^\circ) \\
 &= 1/\sqrt{2} \times [(N_m I_m - N_a I_a \sin \theta_a) \cos(\omega t + \theta) \\
 &\quad - (N_a I_a \cos \theta_a) \sin(\omega t + \theta)] + 1/\sqrt{2} \\
 &\quad \times [(N_m I_m + N_a I_a \sin \theta_a) \cos(\omega t - \theta) \\
 &\quad + (N_a I_a \cos \theta_a) \sin(\omega t - \theta)]
 \end{aligned} \tag{3}$$

Here,  $F(\theta, t)$  denotes magnetomotive force at time  $t$  and position  $\theta$ ,  $F_m(\theta, t)$  denotes main winding magnetomotive force,  $F_a(\theta, t)$  denotes sub winding magnetomotive force,  $N_m i_m$  denotes ampere turn (coil turn number  $\times$  electric current) of main winding,  $N_a i_a$  denotes ampere turn (coil turn number  $\times$  electric current) of sub winding,  $\theta_a$  denotes line frequency ( $= 50$  Hz) and  $\theta_a$  denotes phase difference between main line current and sub line current. The terms of  $\cos(\omega t + \theta)$  and  $\sin(\omega t + \theta)$  in Eq. (3) are revolutionary magnetomotive forces in a backward direction and the terms of  $\cos(\omega t - \theta)$  and  $\sin(\omega t - \theta)$  are revolutionary magnetomotive force in a forward direction.



(a) Unbalanced magnetomotive force of 70 ATs



(b) Without unbalanced magnetomotive force

Fig. 5 Magnetomotive force distribution of 8-pole motor by unbalanced magnetomotive force

The amount of backward magnetomotive force makes varying the distribution of total magnetomotive force according to time and position as shown in Fig. 5 which will amplify torque pulsation (Charles I. Hubert, 2002). Therefore, for this single-phase induction motor, the backward magnetomotive force must be removed in order to be driven as like equilibrium two-phase motor. In order to remove it, the ampere turns of main winding must be equal to that of sub winding and the phase angle between main and sub winding current must be  $90^\circ$  out of phase as given in Eq. (4).

$$\begin{aligned}
 F(\theta, t) &= \sqrt{2} N_m I_m \cos(\omega t - \theta) \\
 &\text{if } N_a I_a = N_m I_m \text{ and } \theta_a = 90^\circ
 \end{aligned} \tag{4}$$

For fan motor, which is dealt with in this paper,

the capacitor of 15  $\mu$ F was used at mock-up sample state and backward occurrence magnetomotive force became 92.7AT (Ampere Turns) from Eq. (3). Therefore in order to act as equilibrium 2-phase motor for this capacitor induction motor, ampere turns of main and sub winding should have equal magnitude and  $90^\circ$  out of phase from Eq. (4).

**2.3 Unbalance minimization of magnetomotive force**

Backward magnetomotive force makes 1-phase induction motor to act as like unbalanced 2-phase motor. This force must decrease as small as possible when the motor is developed. However, mock-up state sample in this paper had backward magnetomotive force of 92.7ATs as referred previous paragraph. The stator winding numbers for main and sub winding had been modified in order to reduce this backward magnetomotive force. Through measurement of current for main and sub winding, the backward magnetomotive force could be calculated. From this procedure, it could reduce backward magnetomotive force to 62ATs.

Figure 6 shows the noise test results for reducing the backward magnetomotive force. It could be seen that the sound pressure level at 2f-line frequency reduced about 10dB. Reducing backward magnetomotive force could reduce motor noise at 2f-line frequency, but the indoor unit still had the peak noise at 2f-line frequency.

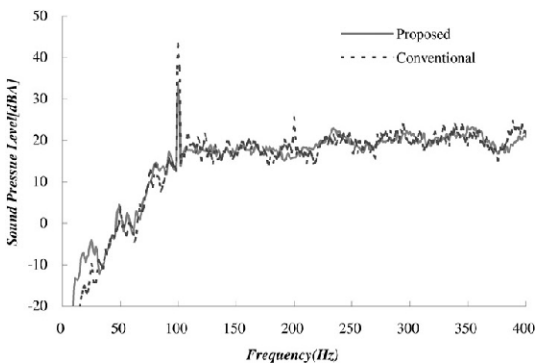


**Fig. 6** Sound pressure level of air conditioner (Experiments) (Conventional : current motor, Proposed : improved motor)

**3. Structural Design of Fan Motor for Reducing 2f-Line Frequency Noise**

The resonance frequency of fan motor was estimated by changing and monitoring power line frequency with frequency converter. In this study, line frequency could be changed from 49 Hz to 54 Hz including usage frequency of 50 Hz by frequency converter. The vibration at 2f-line frequency was measured by FFT analyzer in order to check whether resonance of fan motor was occurred or not. The test results of the vibration for fan motor according to the variation of line frequency were shown in Fig. 7. It can be seen that resonance occurred at 104 Hz and it is 2f-line frequencies of 52 Hz line frequency. The resonance frequency of 104 Hz for the fan motor will cause vibration because this frequency is near to 2f-line frequency of 50 Hz. Therefore, in order to avoid resonance effect at near 100 Hz, design modification was necessary because natural frequency of 104 Hz should be moved further away from 100 Hz. So the normal mode and forced vibration analysis are necessary to modify the natural frequency of the fan motor.

**3.1 Computational analysis of fan motor**

**3.1.1 Normal mode analysis**

If the natural frequency of the fan motor is close to 2f-line frequencies, the noise and vibra-

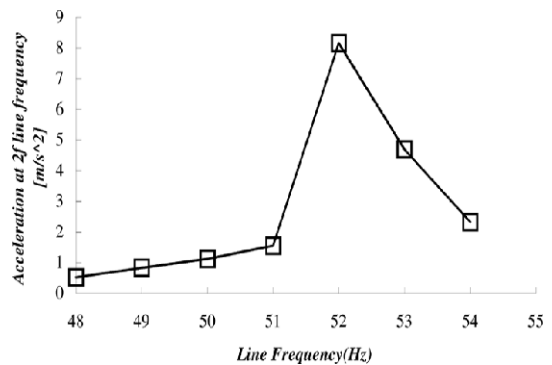


**Fig. 7** Acceleration at 2f-line frequency as changing line frequency (Experiments)

tion of the fan motor will increase excessively because the motor has pulsation torque at 2f-line. Therefore, at the state of fan motor design, it is very important to design fan motor in order that the resonance may not happen at this 2f-line frequency. A model of fan motor system for analysis is given in Fig. 8. Motor stator consists of steel core and copper wire. Because the stiffness of the stator is very large and there is little possibility to happen resonance at low frequency, motor stator is assumed to be a simply lumped mass.

Natural frequency of fan motor can be changed according to the mass and inertia of the rotor, stator and fan as well as axis stiffness. The shape of the fan is usually decided according to air volume, and the size of the motor is decided according to load and speed of revolution. Therefore the mass and moment of inertia of the rotor, stator and fan are difficult to modify. In this study, it is supposed that fan material, motor axis length and diameter are main effective parameters for the change of natural frequencies.

Analysis results are given in Tables 3~5. Tab-

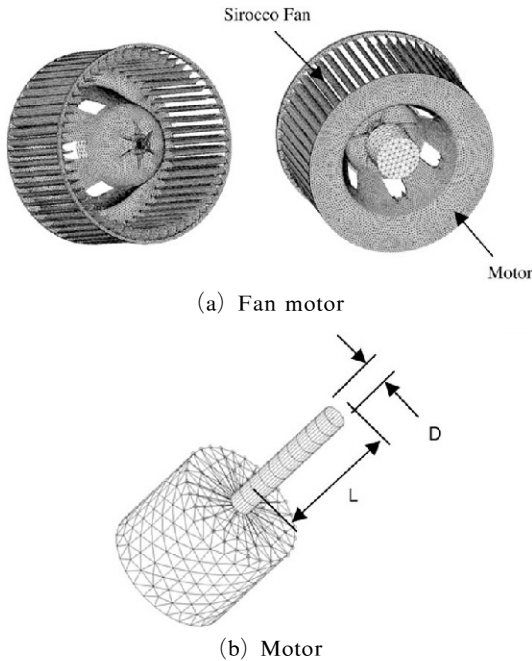


Fig. 8 Finite element modeling of the fan motor system

les 3 and 4 show the changes of natural frequencies with respect to the changes of shaft diameter and length of motor. But the natural frequency at 107.7 Hz near to 2f-line frequency (100 Hz) was not moved so far. Table 5 shows the change of

Table 3 Natural frequencies versus axis length

Order	Natural Frequency [Hz]		
	L=94 mm	L=104 mm	L=84 mm
1	47.5	47.1	47.6
2	48.5	47.6	49.9
3	76.2	74.7	78.4
4	107.7	107.5	107.9
5	123.5	123.5	123.5
6	170	169.8	172.2
7	212	212	212
8	238.5	238.2	238.5

Table 4 Natural frequencies versus axis diameter

Order	Natural Frequency [Hz]		
	D=15 mm	D=13 mm	D=17 mm
1	47.5	46.1	47.6
2	48.5	47.6	49.9
3	76.2	74	77.5
4	107.7	105	108.6
5	123.5	123.5	123.5
6	170	169.9	170
7	212	212	212.6
8	238.5	238.5	238.6

Table 5 Natural frequencies according to fan material

Order	Natural Frequency [Hz]		
	ABS GF 20%	PP	SAN GF 20%
1	47.5	45.9	50.8
2	48.5	47.4	51.7
3	76.2	74.6	85.5
4	107.7	104.6	115.1
5	123.5	119	131.8
6	170	167	181.6
7	212	205	227
8	238.5	230	254

natural frequencies for the fan motor as different fan material. In this case, natural frequency at 107.7 Hz could be moved further. With these results, it could be seen that the change of the fan stiffness is more effective than that of motor axis stiffness in order to change natural frequency of the fan motor,

Figure 9 shows the FRFs of the fan motor obtained by computational analysis for different fan material. Computational analysis was carried out with fan material for different Young’s modules but similar weight with ABS GF 20% used for present sample. The properties of fan material applied in this analysis are given by Table 6. From Fig. 9, replacement the material from ABS GF20% to SAN GF 20% can move natural frequency from 107.7 Hz to 115 Hz. It was estimated that the change of fan material could avoid the resonance phenomenon at the frequency of 100 Hz.

**3.1.2 Forced vibration analysis**

When the fan material was changed from ABS GF 20% to SAN GF 20%, forced vibration analysis

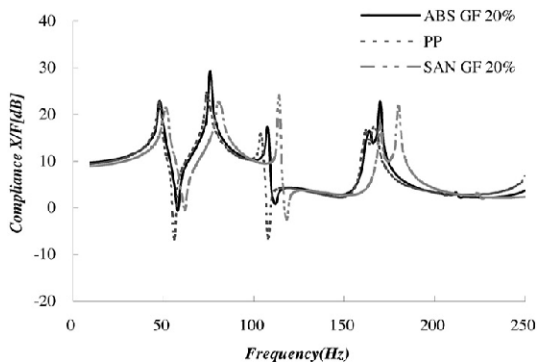
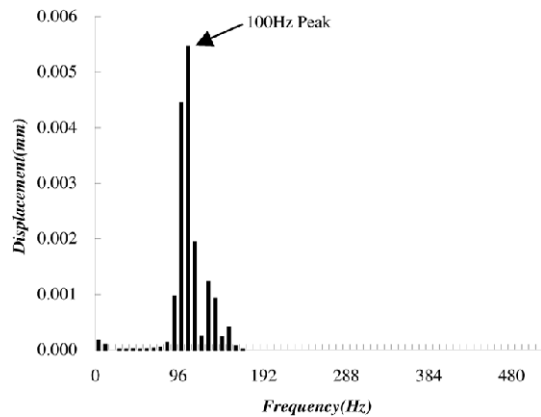


**Fig. 9** FRFs of the fan motor system as alternation of fan materials (FEM)

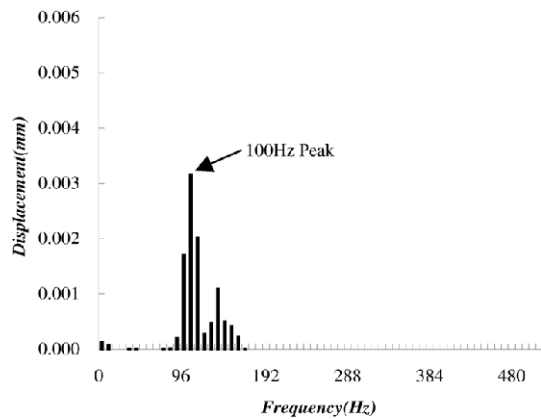
**Table 6** Properties of fan material

	ABS+Glass Fiber 20%	SAN+Glass Fiber 20%	PP
Density (kg/m <sup>3</sup> )	1.18	1.22	1.21
Young’s Modulus (Mpa)	5700	6900	5527.2
Poisson Ratio	0.4	0.4	0.4

was performed in order to examine reduction of the motor vibration. The excitation force of the motor was modeled as described in paragraph 2.1. As the result of previous paragraph, vibration that occurred at 100 Hz could be affected by resonance of the fan motor system and changing fan material could reduce it. Therefore, with finite element modeling that handled in previous paragraph, forced vibration analysis for fan material about ABS GF 20% and SAN GF 20% was carried out. It is assumed that motor excitation force is concentrated at motor spindle. The results of the vibration analysis are given in Fig. 10. When the material of the fan was changed, it could be seen that the vibration displacement level reduced about 70% at 2f-line frequencies due to resonance escaping.



(a) ABS GF 20%



(b) SAN GF 20%

**Fig. 10** Forced vibration as alternation of fan material (FEM)

### 3.2. Experiments

#### 3.2.1 Modal test of fan motor

In order to verify numerical results described in paragraph 3.1, some samples were produced according to the fan material, and the modal tests were performed. Fan motor separated from the air conditioner was used for modal testing. FRFs and natural frequencies by experiment are given in Fig. 11 and Table 7. As test results, it could be seen that 104 Hz mode is rotational mode of the fan motor system and it shows good agreement with those by numerical analysis. And the natural frequency of this rotating mode increased to 117 Hz after fan material alteration, which also fit well relatively with numerical analysis.

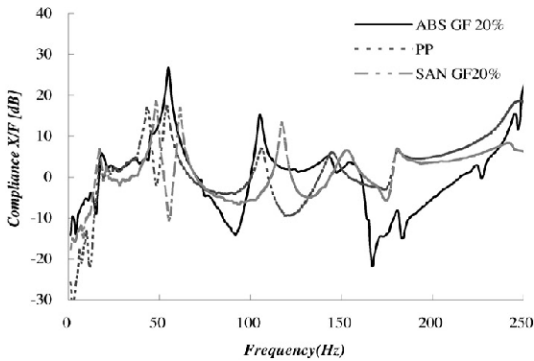


Fig. 11 FRFs of the fan motor system as alternation of fan materials (Experiments)

Table 7 Natural frequencies of fan motor system measured by experiments

Order	Natural Frequency [Hz]		
	ABS GF 20%	PP	SAN GF 20%
1	45	43	48
2	55	54	61
3	76	—	—
4	104	105	117
5	125	—	—
6	145	145	153
7	175	—	—
8	181	—	185
9	217	213	243
10	249	248	273

#### 3.2.2 Vibration and noise test for the fan motor system

The acceleration was measured on the motor base plate by accelerometer, B&K type 4393 because it was hard to measure the fan vibration at the turning time of the fan. Figure 12 shows the measured acceleration on the motor base plate applying ABS GF 20% and SAN GF 20% fan. It could be seen that the acceleration at 2f-line frequency reduced from 10 m/s<sup>2</sup> to 2 m/s<sup>2</sup> by changing fan material. The sound pressure level was also measured as given in Fig. 13. The 2f-line frequency noise reduced about 10dBA when the fan material was changed. Therefore, it was verified that the noise and vibration of the motor could be reduced by resonance escaping of the fan motor system.

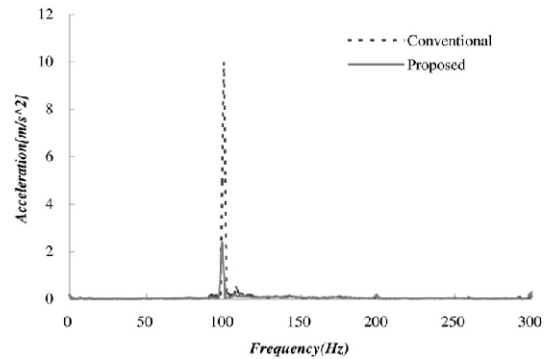


Fig. 12 Acceleration of the motor plate (Experiments) (Conventional : ABS GF 20% Blower, Proposed : SAN GF 20% Blower)

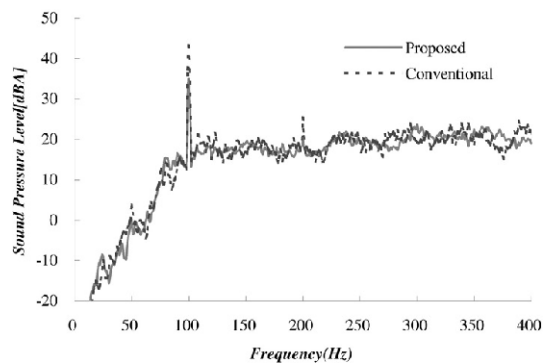


Fig. 13 Sound pressure level of air conditioner (Experiments) (Conventional : ABS GF 20% Blower, Proposed : SAN GF 20% Blower)



#### 4. Discussion

As referred to previous paragraphs, motor noise was produced by electrical problem as well as structural problem. In previous paragraphs, it is verified that reducing the magnetomotive unbalance force of the motor and modifying fan material could reduce motor noise at 2f-line frequency about 10dB. In addition, it could be seen that the motor noise at 2f-line frequency could be reduced about 25dB when these two modifications were applied together as given in Fig. 14. It means that motor noise problem comes from not only electrical problem but also structural one. And also it could be seen that structural and electrical coupling effects must be considered simultaneously when the motor is developed.

#### 5. Conclusions

In order to reduce motor noise at 2f-line frequency, numerical analysis is performed related to electrical and mechanical design. Through the design modification of motor to reduce unbalance magnetomotive force between main and sub winding, sound pressure level at 2f-line frequency could be reduced about 10dB compared to the conventional one. And also through fan material changing from ABS GF 20% to SAN GF 20%,

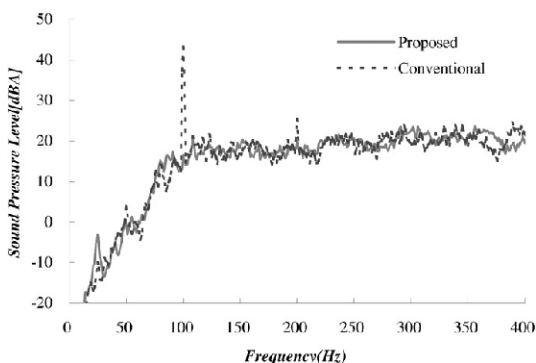


**Fig. 14** Sound pressure level of air conditioner (Experiments) (Conventional: ABS GF 20% Blower and current motor, Proposed: SAN GF 20% Blower and improved motor)

sound pressure level at 2f-line frequency was reduced about 10dB compared to the conventional one. When these two modifications were applied together, sound pressure level at 2f-line frequency could be reduced 25dB compared to the conventional one.

#### References

- Charles I. Hubert, 2002, *Electric Machines : Theory, Operation, Application, Adjustment, and Control* 2nd edition, Prentice-Hall.
- Hamdi, E.S., 1994, *Design of Small Electrical Machine*, John Wiley & Sons, Inc.
- Jeong, W. B., Kim, J. H., Ahn, S. J. and Hwang, S. W., 2002, "Transient Vibration Analysis of a Rotary Compressor Considering the Coupled Effect of Motor," *KSNVE*, Vol. 12, No. 11, pp. 847~855.
- Pareesh C. Sen, 1997, *Principles of Electric Machines and Power Electronics*, John Wiley & Sons, Inc.
- Terrance A. Lettemmaier, Donald W. Novotny and Tomas A. Lipo, 1991, "Single-Phase Induction Motor with an Electrically Controlled Capacitor," *IEEE*, Vol. 27, No. 1, pp. 38~43.
- William R. Finley, 2000, "An Analytic Approach to Solving Motor Vibration Problems," *IEEE*, Vol. 36, No. 5, pp. 1467~1480.
- Williams, Stephen and A.C. Smith, 1999, "A Unified Approach to the Analysis of Single-Phase Induction Motor," *IEEE*, Vol. 35, No. 4, pp. 837~843.
- Yang, B. S. and Son, B. G. 1998, "Stability Analysis of Induction Motor Rotor by Unbalanced Electromagnetic Force," *KSNVE*, Vol. 8, No. 6, pp.1086~1092.
- Yang, J. Y., Kim, J. R., Shin, D. S., Lee, D. J. and Lee, D. H., 2001, "Resonance Noise Control in the Case of Using BLDC Fan Motor," *KSNVE Autumn Conference*, pp. 512~516.
- Yoon, S. B. and Hong, J. P., 1996, "Construction of Equivalent Circuit and Characteristic Analysis of Permanent Split Condenser Induction Motor," *KIEE*, Vol. 45, No. 9, pp. 1247~1254.